CHAPTER

6

The Passive Cable

OUTLINE

Up to this point we have assumed that membrane potential varies in time but not in space. No cell fits this hypothesis exactly and very few cells even fit it approximately. For most neurons resemble dendritic trees or bushes with tens or hundreds of fine thin branches. As each branch resembles, both geometrically and electrically, Lord Kelvin's RC model of the transatlantic telegraph cable, the mathematical study of dendritic branches has come to be called "cable theory". The electrical analogy to Kelvin however only holds in the subthreshold, in fact passive, regime. For Kelvin's cables possessed nothing like our ion channels. In this chapter, our first step into space is softened by the fact that we limit ourselves to uniform, unbranched, passive cables. This permits us to develop analytical and numerical methods with minimal distraction. We will then argue in Chapters 8 and 9 that these survive the extension to active dendritic trees.

We proceed by first deriving the discrete, or compartmental, passive cable equation. We construct its exact (via an eigenvector expansion) and approximate (via the trapezoid rule) solution to current injection. As the compartment size shrinks, and the number of compartments grows, we arrive at the Passive Cable Equation. Methods for studying partial differential equations of this form have been under continuous development for over 150 years. We construct and analyze its exact solution (via an eigenfunction expansion) to current injection in a manner that permits us to reconcile the discrete and continuous formulations. In the final section we consider synaptic input onto a spine appended to the cable. We reverse the process described above by discretizing in space and pursuing a numerical attack.

6.1 THE DISCRETE PASSIVE CABLE EQUATION

We consider a cable of length ℓ and radius a. We choose an integer N and divide the cable into N compartments each of length $dx = \ell/N$ and surface area $2\pi a dx$ and cross sectional area πa^2. We suppose that each compartment is isopotential but permit this potential to vary from compartment to compartment (Figure 6.1).

The only new object here is the coupling resistance between compartments. We express it in terms of R_a in $k\Omega\,cm$, the resistivity of the cytoplasm. The circuit elements are then

$$C = (2\pi a dx)C_m, \quad G = (2\pi a dx)g_{Cl} \quad \text{and} \quad R = dx R_a/(\pi a^2).$$

Current balance at the first node now reads

$$I_{stim} = I_1 + I_2 + I_3 = C(\phi_1 - \phi_0)' + G((\phi_1 - V_{Cl}) - \phi_0)) + (\phi_1 - \phi_2)/R$$

Mathematics for Neuroscientists, Second Edition
DOI: 10.1016/B978-0-12-801895-8.00006-3

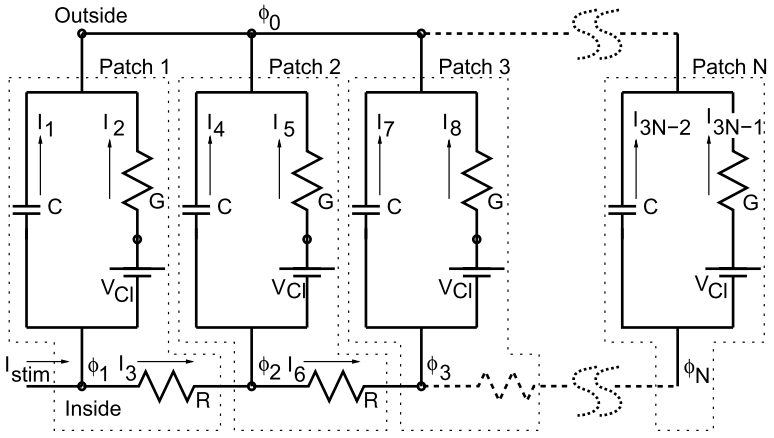

FIGURE 6.1 The compartmentalization of a simple cable.

which, in terms of the relative transmembrane potential

$$v_n \equiv \phi_n - \phi_0 - V_{Cl}, \quad n = 1, \ldots N$$

reads

$$I_{stim} = Cv_1' + Gv_1 + (v_1 - v_2)/R. \tag{6.1}$$

On recalling the time constant, $\tau = C/G$, and defining the 'space constant'

$$\boxed{\lambda \equiv \sqrt{\frac{a}{2R_a g_{Cl}}}} \tag{6.2}$$

division of Eq. (6.1) by G produces

$$\tau v_1' + v_1 - \lambda^2 (v_2 - v_1)/dx^2 = I_{stim}/G. \tag{6.3}$$

Current balance at the second node requires $I_4 + I_5 = I_3 - I_6$, that is

$$Cv_2' + Gv_2 = (v_1 - v_2)/R - (v_2 - v_3)/R \tag{6.4}$$

or, on division by G,

$$\tau v_2' + v_2 - \lambda^2 (v_1 - 2v_2 + v_3)/dx^2 = 0.$$

Similarly, at the nth compartment,

$$Cv_n' + Gv_n = (v_{n+1} - 2v_n + v_{n-1})/R$$

or

$$\tau v_n' + v_n - \lambda^2 (v_{n+1} - 2v_n + v_{n-1})/dx^2 = 0. \tag{6.5}$$

Current balance at the final compartment reads $I_{3N-2} + I_{3N-1} = I_{3N-3}$, that is

$$Cv_N' + Gv_N = (v_{N-1} - v_N)/R$$

or

$$\tau v_N' + v_N - \lambda^2 (v_{N-1} - v_N)/dx^2 = 0. \tag{6.6}$$

Collecting the potentials in the column vector

$$\mathbf{v}(t) = (v_1\ v_2\ \ldots\ v_N)^T$$

we may express the above as

$$\mathbf{v}'(t) = \mathbf{B}\mathbf{v}(t) + \mathbf{f}(t) \tag{6.7}$$

where

$$\mathbf{B} = (\lambda^2\mathbf{S} - \mathbf{I})/\tau, \tag{6.8}$$

$\mathbf{S}$ is the second difference matrix

$$\mathbf{S} = \frac{1}{dx^2}\begin{pmatrix} -1 & 1 & 0 & 0 & \cdots & 0 \\ 1 & -2 & 1 & 0 & \cdots & 0 \\ \cdot & \cdot & \cdot & \cdot & \cdot & \cdot \\ 0 & \cdots & 0 & 1 & -2 & 1 \\ 0 & \cdots & 0 & 0 & 1 & -1 \end{pmatrix} \tag{6.9}$$

and the forcing term is

$$\mathbf{f} = \frac{I_{stim}(t)}{(2\pi adx)C_m}\mathbf{e}_k \quad \text{where} \qquad \mathbf{e}_k \equiv (0\,0\ \ldots\ 0\,1\,0\ \ldots\ 0)^T, \tag{6.10}$$

is associated with current injection into compartment k. Our illustration, Figure 6.1, uses $k = 1$ but we will be interested in the general case. We also presume that each compartment starts from rest, i.e.,

$$\mathbf{v}(0) = 0. \tag{6.11}$$

As in the previous chapter, we solve (6.7) both exactly, via eigenvectors of $\mathbf{B}$, and approximately, via Euler's method.

6.2 EXACT SOLUTION VIA EIGENVECTOR EXPANSION

The second difference matrix, $\mathbf{S}$, is symmetric, i.e., obeys, $\mathbf{S} = \mathbf{S}^T$, and negative semi-definite, i.e., obeys $\mathbf{u}^T\mathbf{S}\mathbf{u} \leq 0$ for every $\mathbf{u} \in \mathbb{R}^N$. As such, its eigenvalues are real and nonpositive (Exercises 1–3). It is also noninvertible and so 0 is an eigenvalue. We may therefore order the eigenvalues as

$$0 = \theta_0 \geq \theta_1 \geq \cdots \geq \theta_{N-1}$$

and denote the corresponding eigenvectors by

$$\mathbf{q}_0,\ \mathbf{q}_1,\ \ldots,\ \mathbf{q}_{N-1}.$$

Together they obey

$$\mathbf{S}\mathbf{q}_n = \theta_n\mathbf{q}_n \tag{6.12}$$

and we note that regardless of whether or not these eigenvalues are distinct (they are) every N-by-N symmetric matrix has an orthonormal basis of N eigenvectors (Exercise 4). That is, the $\mathbf{q}_n$ obey

$$\mathbf{q}_m^T\mathbf{q}_n = \delta_{mn}, \tag{6.13}$$

where δ_{mn} is the Kronecker delta of Eq. (1.4). As $\mathbf{B}$ (recall (6.8)) is simply an affine function of $\mathbf{S}$ it follows that its eigenvalues are

$$z_n = (\lambda^2\theta_n - 1)/\tau, \tag{6.14}$$

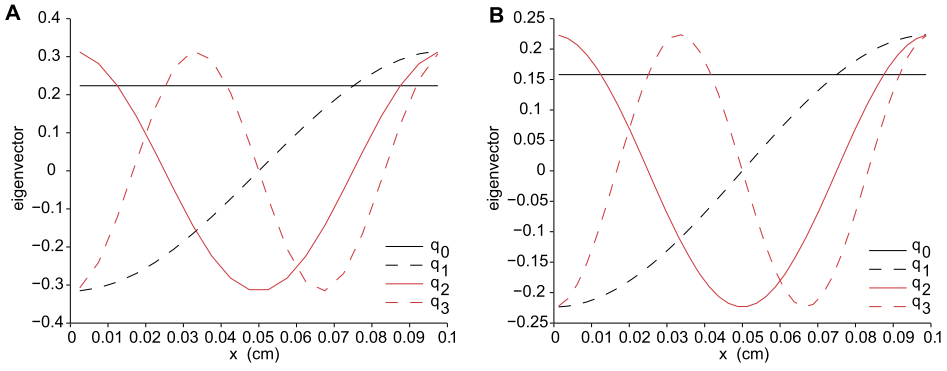

FIGURE 6.2 The first four eigenvectors of $\mathbf{S}$ for $N = 20$ (**A**) and $N = 40$ (**B**) on a cable of length $\ell = 0.1$ cm. These eigenvectors appear to approximate (scalar multiples of) 1, $\cos(x/\ell)$, $\cos(2x/\ell)$ and $\cos(3x/\ell)$ while the associated eigenvalues of $\mathbf{S}$ are very close to integer multiples of $(\pi/\ell)^2$. (`evecS.m`)

and that its eigenvectors remain $\mathbf{q}_n$ (Exercise 5). Recalling Eq. (5.19) it remains to solve $\mathbf{Qc}(t) = \mathbf{f}(t)$ where

$$\mathbf{Q} = (\mathbf{q}_0\ \mathbf{q}_1\ \cdots\ \mathbf{q}_{N-1}) \tag{6.15}$$

is the N-by-N matrix composed of the orthonormal eigenvectors of $\mathbf{S}$. Now by orthonormality we note (Exercise 6) that $\mathbf{Q}^{-1} = \mathbf{Q}^T$ and so, recalling the $\mathbf{f}$ of (6.10),

$$\mathbf{c}(t) = \frac{I_{stim}(t)}{2\pi a dx C_m}\mathbf{Q}^T\mathbf{e}_k = \frac{I_{stim}(t)}{2\pi a dx C_m}(q_{0,k}\ q_{1,k}\ \cdots\ q_{N-1,k})^T.$$

We see that $\mathbf{Q}^T\mathbf{e}_k$ is comprised of the kth component of each of the eigenvectors. Now, following the lead of Eq. (5.21), we conclude that

$$\boxed{\mathbf{v}(t) = \frac{N}{2\pi a\ell C_m}\sum_{n=0}^{N-1}\mathbf{q}_n q_{n,k}\int_0^t I_{stim}(s)\exp((t-s)z_n)\,ds.} \tag{6.16}$$

Although cumbersome in appearance, this expression is the sum of elementary objects that should be familiar from our isopotential work back in Chapter 3. More precisely, Eq. (6.16) states that $\mathbf{v}(t)$ is a weighted sum of convolutions, $I_{stim} \star \exp(tz_n)$, that differ from the isopotential case, Eq. (3.2), only in the sense that the membrane time constant, τ, has been replaced with $-1/z_n$. This difference in fact permits us to interpret the N eigenvalues, z_n, as a sequence of decay rates for the N-compartment cable. These rates however are not specific to individual compartments but instead to individual eigenvectors, $\mathbf{q}_n$, for these (together with the signature, $q_{n,k}$, of the stimulus location) serve as the weights for the individual convolutions. We will soon derive exact expressions for the z_n and $\mathbf{q}_n$. For now, we invoke `eig` in MATLAB and illustrate in Figure 6.2 the first few eigenvectors as "functions" of cable length.

As a concrete application of (6.16) let us consider the cable

$$\ell = 1\text{ mm},\quad a = 1\ \mu\text{m},\quad C_m = 1\ \mu\text{F/cm}^2,\quad g_{Cl} = 1/15\text{ mS/cm}^2,\quad R_a = 0.3\ \text{k}\Omega\,\text{cm} \tag{6.17}$$

and suppose that $I_{stim}(t)$ takes the constant value I_0. In this case, (6.16) reduces to

$$\mathbf{v}(t) = \frac{I_0 N}{2\pi a\ell C_m}\sum_{n=0}^{N-1}\frac{\mathbf{q}_n q_{n,k}}{z_n}(\mathrm{e}^{z_n t} - 1)$$

which, as $t \to \infty$, converges to

$$\mathbf{v}_\infty = \frac{-I_0 N}{2\pi a\ell C_m}\sum_{n=0}^{N-1}\frac{\mathbf{q}_n q_{n,k}}{z_n} \tag{6.18}$$

as illustrated in Figure 6.3A.

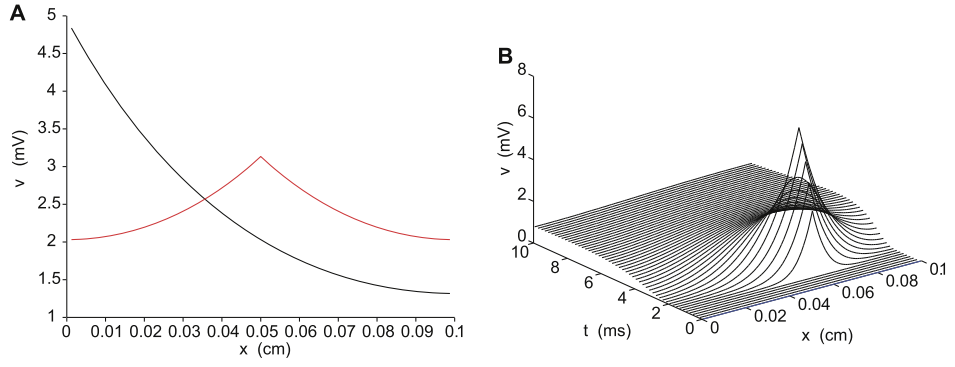

FIGURE 6.3 **A**. The steady-state solution, Eq. (6.18), for the cable parameters in (6.17), $I_0 = 1$ nA, $N = 41$ and a stimulus at compartments $k = 1$, black, or $k = 21$, red. (`steady.m`) **B**. Dynamic response, Eq. (6.20), of the same cable to the stimulus of Eq. (6.19), $I_0 = 10$ nA, $t_1 = 1$ and $t_2 = 2$ ms at $x = 0.06$ cm, with $N = 100$. (`eigcab.m`)

As a second example, if we inject the pulse

$$I_{stim}(t) = I_0 \mathbb{1}_{(t_1,t_2)}(t) \tag{6.19}$$

at compartment k then Eq. (6.16) takes the form

$$\mathbf{v}(t) = \frac{-I_0 N}{2\pi a \ell C_m} \sum_{n=0}^{N-1} \frac{\mathbf{q}_n q_{n,k}}{z_n} (e^{\max(t-t_2,0)z_n} - e^{\max(t-t_1,0)z_n}) \tag{6.20}$$

as presented in Figure 6.3B. We will establish below that the attenuation in the steady response away from the site of stimulation is of the form $\exp(-x/\lambda)$. In other words, the response drops by factor of $1/e$ within one space constant, λ, from the stimulus. Note that $\lambda = 0.05$ cm for the cable specified in Eq. (6.17).

6.3 NUMERICAL METHODS

We formulate three straightforward marching schemes for the

$$\text{stimulus} \quad \mathsf{f}^j = \mathbf{f}((j-1)dt) \quad \text{and response} \quad \mathsf{v}^j \approx \mathbf{v}((j-1)dt)$$

associated with the discrete cable equation, Eq. (6.7). The forward Euler scheme reads

$$(\mathsf{v}^j - \mathsf{v}^{j-1})/dt = \mathbf{B}\mathsf{v}^{j-1} + \mathsf{f}^{j-1}, \quad \text{i.e.,} \quad \mathsf{v}^j = (\mathbf{I} + dt\mathbf{B})\mathsf{v}^{j-1} + dt\,\mathsf{f}^{j-1} \tag{6.21}$$

while the backward Euler scheme requires

$$(\mathsf{v}^j - \mathsf{v}^{j-1})/dt = \mathbf{B}\mathsf{v}^j + \mathsf{f}^j, \quad \text{i.e.,} \quad (\mathbf{I} - dt\mathbf{B})\mathsf{v}^j = \mathsf{v}^{j-1} + dt\,\mathsf{f}^j \tag{6.22}$$

and the trapezoid scheme that

$$\mathsf{v}^j - \mathsf{v}^{j-1} = \mathbf{B}(\mathsf{v}^j + \mathsf{v}^{j-1})dt/2 + (\mathsf{f}^j + \mathsf{f}^{j-1})dt/2$$

or

$$(\mathbf{I} - (dt/2)\mathbf{B})\mathsf{v}^j = (\mathbf{I} + (dt/2)\mathbf{B})\mathsf{v}^{j-1} + (dt/2)(\mathsf{f}^j + \mathsf{f}^{j-1}). \tag{6.23}$$

At first sight it appears that (6.23) requires one additional (over Backward Euler) matrix-vector product per iteration. To see that this is not the case note that (6.23) is equivalent to

$$\text{set} \quad \mathbf{r}^2 = (dt/2)(\mathsf{f}^2 + \mathsf{f}^1)$$

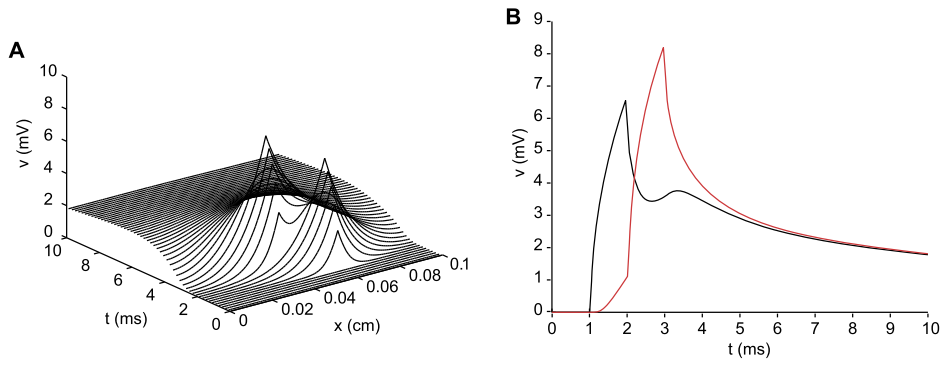

FIGURE 6.4 Response of the cable of Eq. (6.17), as revealed by the Trapezoid Scheme ($dx = 1$ μm, $dt = 0.05$ ms), Eq. (6.24), to the double stimulation in Eq. (6.25), $I_0 = 100$ pA, $x_1 = 0.06$ cm, $t_{1,1} = 1$, $t_{2,1} = 2$ ms and $x_2 = 0.04$, $t_{1,2} = 3$, $t_{2,2} = 4$. The proximity of the two stimuli, in both space and time, leads to significant boosting of the latter response. **A**. The full space–time response. **B**. The response in time at the early site, x_1 (black), and the late site, x_2, (red). (`trapcab.m`)

and for $j = 2, 3, \ldots,$

$$\text{solve } (\mathbf{I} - (dt/2)\mathbf{B})\mathtt{v}^j = \mathbf{r}^j \quad \text{and set } \mathbf{r}^{j+1} = 2\mathtt{v}^j - \mathbf{r}^j + (dt/2)(\mathtt{f}^{j+1} + \mathtt{f}^j). \tag{6.24}$$

Regarding implementation, we note that both (6.22) and (6.24) require the solution of a linear system of equations at each step in time. As the matrix in each case **does not** depend on j we may decompose it, once and for all, into lower and upper triangular factors. This provides significant acceleration of the associated time marching scheme. MATLAB constructs these factors (recall Exercise 4.2) via $[\mathtt{L}, \mathtt{U}] = \mathtt{lu(speye(N) - (dt/2)B)}$ and so the solution of (6.24) is reduced to two triangular solves, $\mathbf{v}^j = \mathbf{U}\backslash(\mathbf{L}\backslash\mathbf{r}^j)$. We have coded this in `trapcab.m` and illustrate it in Figure 6.4 in the case of dual injection

$$\mathbf{I}_{stim}(t) = I_0\{\mathbf{e}_{c_1}\mathbb{1}_{(t_{1,1},t_{2,1})} + \mathbf{e}_{c_2}\mathbb{1}_{(t_{1,2},t_{2,2})}\} \tag{6.25}$$

at compartments c_1 and c_2. These compartment indices are computed from the specified cable length, ℓ, space-step, dx, and stimulation locations x_1 and x_2 via $c_i = \mathtt{round}(x_i/dx)$.
We next compare the accuracy of the Trapezoid and Backward Euler schemes, under the assumption that

$$\mathbf{f}(t) = \frac{\mathrm{e}^{-t} - \mathrm{e}^{-2t}}{10C_m 2\pi a}\mathbf{q}_1.$$

In this case, the exact solution, recall Eq. (6.16), is

$$\mathbf{v}^{(ex)}(t) = \frac{\mathrm{e}^{z_1 t} - \mathrm{e}^{-t}(z_1+2) + \mathrm{e}^{-2t}(z_1+1)}{10C_m 2a\pi(z_1+1)(z_1+2)}\mathbf{q}_1$$

and so, with sc denoting either the Backward Euler or Trapezoid scheme, we compute the maximum absolute error by

$$E(dt, sc) \equiv \max_j \max_n |\mathtt{v}_n^j(sc) - \mathbf{v}_n^{(ex)}((j-1)dt)|$$

and illustrate our findings in Figure 6.5.

6.4 THE PASSIVE CABLE EQUATION

We have examined the role of the time step dt in our resolution of the voltage response of the discrete passive cable. We now investigate the role of the space step, dx. To begin, we let the number, N, of compartments approach

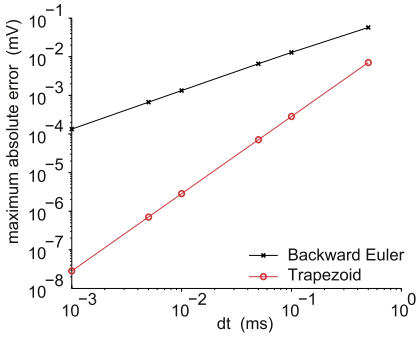

FIGURE 6.5 Illustration of the fact that Backward Euler is accurate to $O(dt)$ while Trapezoid is accurate to $O(dt^2)$. Number of compartments, $N = 100$. (`cndrive.m, cnpfib.m`)

∞. As $dx = \ell/N$ this limit is equivalent to $dx \to 0$. In this limit we will pass from a spatially discrete set of potentials, $\mathbf{v}(t) = (v_1(t)\ v_2(t)\ \cdots\ v_N(t))^T$, to a continuous set of potentials, $v(x,t),\ 0 \le x \le \ell$. For small dx we expect $v((n-1/2)dx,t)$ to be the potential at the center of the nth compartment, i.e., $v_n(t)$. To begin, we will suppose that current is injected into the first compartment. Discrete current balance at the left end, Eq. (6.1), in terms of our approximation $v((n-1/2)dx,t) \approx v_n(t)$, takes the form

$$C_m(2\pi a dx)\frac{\partial v}{\partial t}(dx/2,t) + g_{Cl}(2\pi a dx)v(dx/2,t) - \frac{\pi a^2}{R_a}\frac{v(3dx/2,t) - v(dx/2,t)}{dx} = I_{stim}(t). \tag{6.26}$$

As dx approaches zero this takes the form

$$\frac{\partial v}{\partial x}(0,t) = -\frac{R_a}{\pi a^2}I_{stim}(t), \qquad 0 < t. \tag{6.27}$$

By identical reasoning at the cable's far end, we find

$$\frac{\partial v}{\partial x}(\ell,t) = 0, \qquad 0 < t. \tag{6.28}$$

Now at an interior point, x, we deduce from Eq. (6.5) that

$$\tau\frac{\partial v}{\partial t}(x,t) + v(x,t) - \lambda^2\frac{v(x+dx,t) - 2v(x,t) + v(x-dx,t)}{dx^2} = 0 \tag{6.29}$$

which, as dx approaches zero becomes (Exercise 10)

$$\boxed{\tau\frac{\partial v}{\partial t}(x,t) + v(x,t) - \lambda^2\frac{\partial^2 v}{\partial x^2}(x,t) = 0,} \quad 0 < x < \ell, \quad 0 < t. \tag{6.30}$$

Finally, if the entire cable is initially at rest then

$$v(x,0) = 0 \quad 0 < x < \ell. \tag{6.31}$$

The cable equation, (6.30), together with its boundary conditions, (6.27)–(6.28), and initial condition, (6.31), is an instance of a well studied class of partial differential equations.

The steady-state solution to end-point stimulus. To begin, we suppose a constant current stimulus, $I_{stim}(t) = I_0$, and search for the steady-state solution $v_\infty(x) \equiv v(x, t \to \infty)$. In this limit we may ignore the time-derivative in the cable equation, (6.30), and so find that v_∞ must obey the ordinary differential equation

$$\lambda^2 v_\infty''(x) = v_\infty(x), \tag{6.32}$$

subject to the boundary conditions,

$$v'_\infty(0) = -\frac{R_a}{\pi a^2} I_0, \quad v'_\infty(\ell) = 0. \tag{6.33}$$

In Exercise 11 the reader will construct the solution

$$v_\infty(x) = \frac{I_0 R_a \lambda \cosh((\ell - x)/\lambda)}{\pi a^2 \sinh(\ell/\lambda)} \tag{6.34}$$

and contrast it to the discrete steady-state, (6.18), computed in the previous section. This function takes its maximum value at the site, $x = 0$, of stimulation, and so it is natural to define the associated input resistance

$$R_{in}(0) \equiv \frac{v_\infty(0)}{I_0} = \frac{R_a \lambda \cosh(\ell/\lambda)}{\pi a^2 \sinh(\ell/\lambda)}. \tag{6.35}$$

We note that this decreases with cable length ℓ.

The transient solution to end-point stimulus. We now return to the full cable equation and derive an eigenrepresentation of v reminiscent of (6.16). The basic idea is to **separate variables**, i.e., to suppose that v may be written as a product of univariate functions of space and time. Note that if we substitute the guess

$$v(x,t) \stackrel{?}{=} q(x)p(t) \tag{6.36}$$

into the cable equation, Eq. (6.30), we find

$$\tau q(x)p'(t) + q(x)p(t) = \lambda^2 q''(x)p(t).$$

If we now divide this through by qp we arrive at

$$\tau p'(t)/p(t) + 1 = \lambda^2 q''(x)/q(x).$$

Now note that the function on the right depends solely on x while that on the left depends solely on t. Taking then an x derivative of each side we find that $q''(x)/q(x)$ must be constant. We write this constant as ϑ and so arrive at

$$q''(x) = \vartheta q(x), \quad 0 < x < \ell. \tag{6.37}$$

This eigenvalue problem will be the infinite dimensional analog of the matrix eigenvalue problem, (6.12), once we prescribe the domain of permissible q. More precisely, it remains to translate the top and bottom rows of $\mathbf{S}$ into boundary conditions on (6.37). Recalling (6.28) it seems 'natural' to prescribe $q'(\ell) = 0$. At the near end, where I_{stim} is applied, the correct prescription is less obvious. If q is however to be an eigenfunction of d^2/dx^2 we expect it to be independent of the stimulus. An indication of the 'right' way forward can be glimpsed from Figure 6.2. The 'cosinesque' functions indeed suggest the prescription $q'(0) = 0$. Appending

$$q'(0) = q'(\ell) = 0 \tag{6.38}$$

to (6.37) we arrive, via Exercise 12, at the eigenvalues and eigenfunctions

$$\begin{aligned} &\vartheta_0 = 0, \quad q_0(x) = 1/\sqrt{\ell}, \\ &\vartheta_n = -n^2\pi^2/\ell^2, \quad q_n(x) = \sqrt{2/\ell}\cos(n\pi x/\ell), \ n = 1, 2, \ldots \end{aligned} \tag{6.39}$$

We note that these q_n are orthonormal in the sense that

$$\int_0^\ell q_n(x) q_m(x)\, dx = \delta_{mn}. \tag{6.40}$$

Finding many q we modify our naive guess, (6.36), to

$$v(x,t) = \sum_{n=0}^{\infty} q_n(x)\, p_n(t) \tag{6.41}$$

and proceed to determine the p_n. First, thanks to orthonormality, we may multiply each side of (6.41) by an eigenfunction, integrate, and arrive at

$$p_n(t) = \int_0^\ell q_n(x) v(x,t)\, dx. \tag{6.42}$$

We now use the cable equation to derive an ordinary differential equation for each of the p_n.

$$\begin{aligned}\tau p_n'(t) &= \tau \int_0^\ell q_n(x) \frac{\partial v}{\partial t}(x,t)\, dx = \int_0^\ell q_n(x) \left(\lambda^2 \frac{\partial^2 v}{\partial x^2}(x,t) - v(x,t) \right) dx \\ &= \lambda^2 \int_0^\ell q_n(x) \frac{\partial^2 v}{\partial x^2}(x,t)\, dx - p_n(t).\end{aligned} \tag{6.43}$$

We unravel the remaining integral by twice integrating by parts. Namely,

$$\begin{aligned}\int_0^\ell q_n(x) \frac{\partial^2 v}{\partial x^2}(x,t)\, dx &= q_n(x) \frac{\partial v}{\partial x}(x,t) \Big|_{x=0}^{\ell} - \int_0^\ell q_n'(x) \frac{\partial v}{\partial x}(x,t)\, dx \\ &= -q_n(0) \frac{\partial v}{\partial x}(0,t) - \int_0^\ell q_n'(x) \frac{\partial v}{\partial x}(x,t)\, dx \\ &= -q_n(0) \frac{\partial v}{\partial x}(0,t) - q_n'(x) v(x,t) \Big|_{x=0}^{\ell} + \int_0^\ell q_n''(x) v(x,t)\, dx \\ &= q_n(0) R_2 I_{stim}(t)/(\pi a^2) + \vartheta_n p_n(t).\end{aligned}$$

It follows that each $p_n(t)$ obeys the initial value problem

$$\tau p_n'(t) + (1 - \lambda^2 \vartheta_n) p_n(t) = \lambda^2 q_n(0) R_a I_{stim}(t)/(\pi a^2), \quad p_n(0) = 0. \tag{6.44}$$

We note that the time varying stimulus now appears as a driving term in the time varying component of v. This equation is exactly the one we derived back in Chapter 2 for the isopotential cell. Recalling Eq. (3.2), we find

$$p_n(t) = \frac{q_n(0)}{2\pi a C_m} \int_0^t I_{stim}(s) \exp((t-s)\zeta_n)\, ds$$

where

$$\zeta_n = (\lambda^2 \vartheta_n - 1)/\tau$$

and so, returning to Eq. (6.41), we conclude that

$$\boxed{v(x,t) = \sum_{n=0}^{\infty} \frac{q_n(0) q_n(x)}{C_m 2a\pi} \int_0^t I_{stim}(s) \exp((t-s)\zeta_n)\, ds.} \tag{6.45}$$

This is identical in structure to the solution, Eq. (6.16), of the discrete passive cable. We will investigate in Exercise 13 the sense in which this sum converges.

The transient solution to interior-point stimulus. In the case that we deliver the stimulus at $x = x_s$ the discrete current balance there takes the form

$$(2\pi a dx) \left(C_m \frac{\partial v}{\partial t}(x_s,t) + g_{Cl} v(x_s,t) \right) - \frac{\pi a^2}{R_a} \frac{v(x_s+dx,t) - 2v(x_s,t) + v(x_s-dx,t)}{dx} = I_{stim}(t),$$

or, after division by $2\pi a dx$,

$$\tau \frac{\partial v}{\partial t}(x_s,t) + v(x_s,t) - \lambda^2 \frac{v(x_s+dx,t) - 2v(x_s,t) + v(x_s-dx,t)}{dx^2} = \frac{I_{stim}(t)}{2\pi a dx g_{Cl}}.$$

As we pass to the limit we see that the spatial "footprint" of the injection is of length dx and magnitude $1/dx$. Recalling our work in Chapter 3, in particular Eq. (3.6), we see that this footprint converges to the delta function centered at x_s. It follows that our cable equation now takes the form

$$\tau \frac{\partial v}{\partial t}(x,t) + v(x,t) - \lambda^2 \frac{\partial^2 v}{\partial x^2}(x,t) = I_{stim}(t)\delta(x-x_s)/(2\pi a g_{Cl}) \tag{6.46}$$

and that *both* ends are now sealed, i.e.,

$$\frac{\partial v}{\partial x}(0,t) = \frac{\partial v}{\partial x}(\ell,t) = 0.$$

To solve (6.46) we retrace each of the steps in our previous derivation and find that (6.45) retains its form but shifts its attention from $q_n(0)$ to $q_n(x_s)$. That is, the solution to (6.46) is

$$\boxed{v(x,t) = \sum_{n=0}^{\infty} \frac{q_n(x_s)q_n(x)}{C_m 2a\pi} \int_0^t I_{stim}(s)\exp((t-s)\zeta_n)\,ds,} \tag{6.47}$$

where q_n and ζ_n are exactly as above.

The steady-state solution given interior-point current injection. If I_{stim} is held constant at I_0 then the potential will approach the solution of the steady-state equation

$$v_\infty(x) - \lambda^2 v_\infty''(x) = I_0\delta(x-x_s)/(2\pi a g_{Cl}), \tag{6.48}$$

subject to $v_\infty'(0) = v_\infty'(\ell) = 0$. Arguing as in Exercise 11 we find that v_∞ is proportional to $\cosh(x/\lambda)$ for $x < x_s$ and proportional to $\cosh((\ell-x)/\lambda)$ for $x > x_s$. The ambiguity is resolved by enforcing continuity of v_∞ and current balance at x_s. The latter follows from integrating Eq. (6.48) in a vanishingly small interval about x_s. More precisely,

$$-\lambda^2(v_\infty'(x_s^+) - v_\infty'(x_s^-)) = I_0/(2\pi a g_{Cl}).$$

These observations lead us to

$$v_\infty(x) = \frac{I_0}{2\pi a\lambda g_{Cl}} \frac{1}{\sinh(\ell/\lambda)} \begin{cases} \cosh(x/\lambda)\cosh((\ell-x_s)/\lambda) & \text{if } 0 \le x \le x_s \\ \cosh(x_s/\lambda)\cosh((\ell-x)/\lambda) & \text{if } x_s \le x \le \ell. \end{cases} \tag{6.49}$$

This attains its maximum at x_s, the site of stimulation, and so the associated input resistance takes the form

$$R_{in}(x_s) \equiv \frac{v_\infty(x_s)}{I_0} = \frac{1}{2\pi a\lambda g_{Cl}} \frac{\cosh(x_s/\lambda)\cosh((\ell-x_s)/\lambda)}{\sinh(\ell/\lambda)}. \tag{6.50}$$

We graph this in Figure 6.6 for the cable at hand.

Reconciling the discrete and the continuous. Given the eigenfunctions, Eq. (6.39), of the cable we might guess that the jth component of the nth eigenvector of the discrete cable (neglecting the normalization constant) is the value that the nth eigenfunction takes at the center of the jth compartment. That is,

$$q_{n,j} = q_n((j-1/2)dx) = \cos(n\pi(j-1/2)/N). \tag{6.51}$$

This indeed agrees with the eigenvectors of Figure 6.2 and, on substituting Eq. (6.51) into Eq. (6.12) we indeed find equality so long as the associated compartmental eigenvalues obey

$$\theta_n = -4(N/\ell)^2 \sin^2(n\pi/(2N)). \tag{6.52}$$

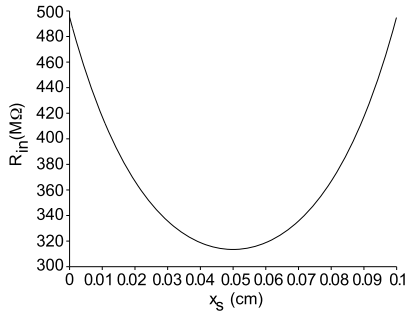

FIGURE 6.6 The input resistance, R_{in}, Eq. (6.50), as a function of stimulus site, x_s, for the cable described by Eq. (6.50). We see a marked increase in R_{in} as the stimulus moves away from the center and toward a sealed end. (`Rinxs.m`)

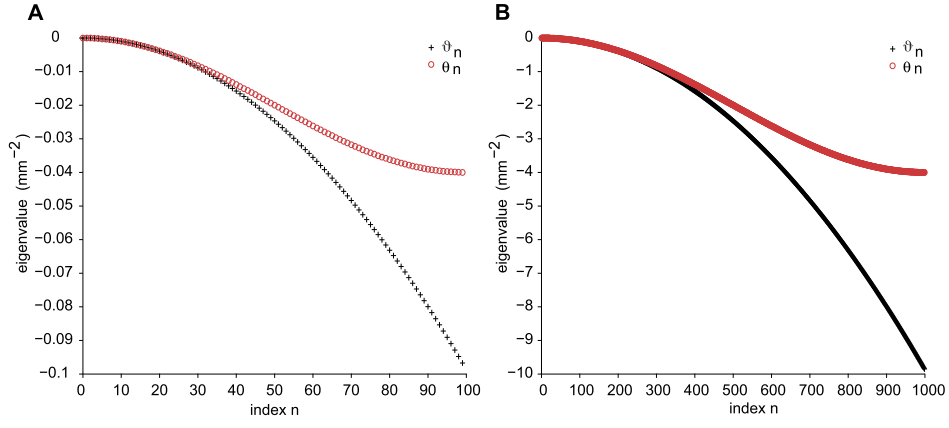

FIGURE 6.7 The eigenvalues of the discrete, θ_n, and continuous, ϑ_n, cable of length $\ell = 1$ mm for $N = 100$ and $dx = 10$ μm (**A**), and $N = 1000$ and $dx = 1$ μm (**B**). (`thvsvth.m`)

This is welcome news in that we now have exact knowledge of every term in the solution, Eq. (6.16), to the discrete cable equation. In addition, by contrasting θ_n and ϑ_n we see that the eigenvalues of the discrete cable accurately capture only the lowest $N/3$ of the true eigenvalues, as illustrated in Figure 6.7.

6.5 SYNAPTIC INPUT

If rather than current injection we instead have synaptic input, with conductance g_{syn} (in units of mS) and reversal potential V_{syn} (in mV), at x_s then the cable equation, Eq. (6.46), takes the form

$$\tau \frac{\partial v}{\partial t}(x,t) + v(x,t) - \lambda^2 \frac{\partial^2 v}{\partial x^2}(x,t) + c_{syn}(t)(v(x,t) - v_{syn})\delta(x - x_s) = 0 \tag{6.53}$$

where

$$v_{syn} \equiv V_{syn} - V_{Cl} \quad \text{and} \quad c_{syn}(t) \equiv \frac{g_{syn}(t)}{2\pi a g_{Cl}}.$$

The time dependence of g_{syn} here defeats the separation of variables that led to our clean representations in (6.45) and (6.47). We turn therefore to approximate means. We choose a spatial step, dx, and a time step, dt, and build a consistent linear system for the discrete potentials

$$v_n^j \approx v((n - 1/2)dx, (j-1)dt), \quad n = 1, 2, \ldots, N \tag{6.54}$$

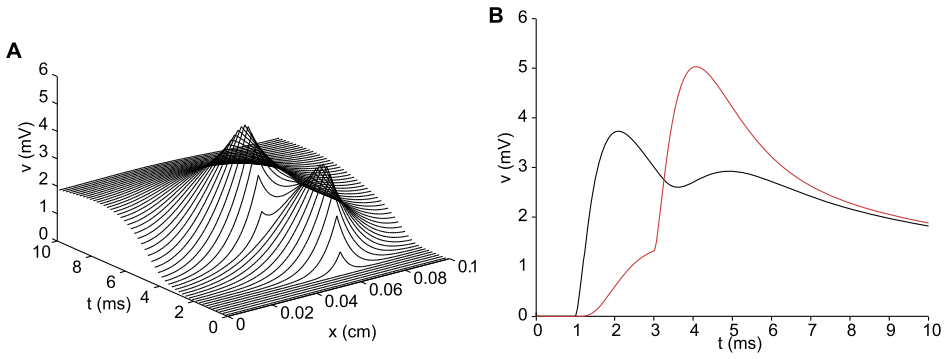

FIGURE 6.8 Response to α-function synaptic input with $\overline{g}_{syn} = 100$ nS, $\tau_\alpha = 1/2$ ms at $x = 0.06$ cm at $t_1 = 1$ ms and $x = 0.04$ at $t_1 = 3$. (`trapcabsyn.m`)

where $N = \ell/dx$ is the number of compartments and $(n-1/2)dx$ is the midpoint of the nth compartment. With regard to Eq. (6.53) we approximate the second space derivative via action of our second difference matrix, $\mathbf{S}$, and the time derivative by the trapezoid rule. If the synapse is located at compartment k then our discrete system takes the form

$$2\tau\frac{\mathtt{v}_n^j-\mathtt{v}_n^{j-1}}{dt}+\mathtt{v}_n^j+\mathtt{v}_n^{j-1}-\lambda^2\frac{\mathtt{v}_{n+1}^j-2\mathtt{v}_n^j+\mathtt{v}_{n-1}^j}{dx^2}-\lambda^2\frac{\mathtt{v}_{n+1}^{j-1}-2\mathtt{v}_n^{j-1}+\mathtt{v}_{n-1}^{j-1}}{dx^2}$$
$$+(\mathtt{c}^j\mathtt{v}_n^j+\mathtt{c}^{j-1}\mathtt{v}_n^{j-1})\delta_{nk}=(\mathtt{c}^j+\mathtt{c}^{j-1})v_{syn}\delta_{nk} \tag{6.55}$$

where $\mathtt{c}^j = c_{syn}((j-1)dt)/dx$. Here $1/dx$ denotes the height of the discrete Dirac delta associated with the synaptic footprint at compartment k. We express Eq. (6.55) more compactly as

$$((2\tau/dt)\mathbf{I}-\mathbf{B}+\mathtt{c}^j\mathbf{e}_k\mathbf{e}_k^T)\mathtt{v}^j=((2\tau/dt)\mathbf{I}+\mathbf{B}-\mathtt{c}^{j-1}\mathbf{e}_k\mathbf{e}_k^T)\mathtt{v}^{j-1}+(\mathtt{c}^j+\mathtt{c}^{j-1})v_{syn}\mathbf{e}_k \tag{6.56}$$

where $\mathbf{B}=\lambda^2\mathbf{S}-\mathbf{I}$ and $\mathtt{v}^j=(\mathtt{v}_1^j\ \mathtt{v}_2^j\ \cdots\ \mathtt{v}_N^j)^T$. We solve Eq. (6.56) by setting $\mathtt{v}^1=0$ and then

$$\mathbf{r}^j\equiv\begin{cases}(\mathtt{c}^1+\mathtt{c}^2)v_{syn}\mathbf{e}_k & \text{if } j=2,\\ 2(2\tau/dt)\mathtt{v}^{j-1}-\mathbf{r}^{j-1}+(\mathtt{c}^j+\mathtt{c}^{j-1})v_{syn}\mathbf{e}_k & \text{if } j>2,\end{cases}\quad\text{and}\quad((2\tau/dt)\mathbf{I}-\mathbf{B}+\mathtt{c}^j\mathbf{e}_k\mathbf{e}_k^T)\mathtt{v}^j=\mathbf{r}^j.$$

We note that this procedure generalizes easily to the polysynaptic case

$$\tau\frac{\partial v}{\partial t}(x,t)+v(x,t)-\lambda^2\frac{\partial^2 v}{\partial x^2}(x,t)=\sum_{m=1}^{M}c_{syn,m}(t)(v_{syn,m}-v(x,t))\delta(x-x_{s,m}) \tag{6.57}$$

where $c_{syn,m}(t)$ is the normalized conductance change associated with a synapse at $x_{s,m}$ with relative reversal potential $v_{syn,m}$. We have coded its solution in `trapcabsyn.m` and illustrate its use in Figure 6.8.

On cortical pyramidal cells and several other neuron types, the vast majority of excitatory synaptic contacts are made not onto the soma or dendrites but onto the heads of small spines, as illustrated in Figure 6.9.

We suppose that the spine head is isopotential, with transmembrane potential W, and we describe the spine geometry in terms of ℓ_{sn}, the spine neck length, a_{sn}, the spine neck radius, and A_{sh}, the surface area of the spine head. We adopt the typical values

$$\ell_{sn}=1\ \mu\text{m},\quad a_{sn}=0.1\ \mu\text{m},\quad A_{sh}=1\ \mu\text{m}^2. \tag{6.58}$$

The spine neck presents an axial resistance while the spine head sports both a membrane capacitance and conductance and a synapse. In particular,

$$R_{sn}=\ell_{sn}R_a/(\pi a_{sn}^2),\quad G_{sh}=g_{Cl}A_{sh}\quad\text{and}\quad g_{syn}=\overline{g}_{syn}(t)\rho_{syn}A_{sh}$$

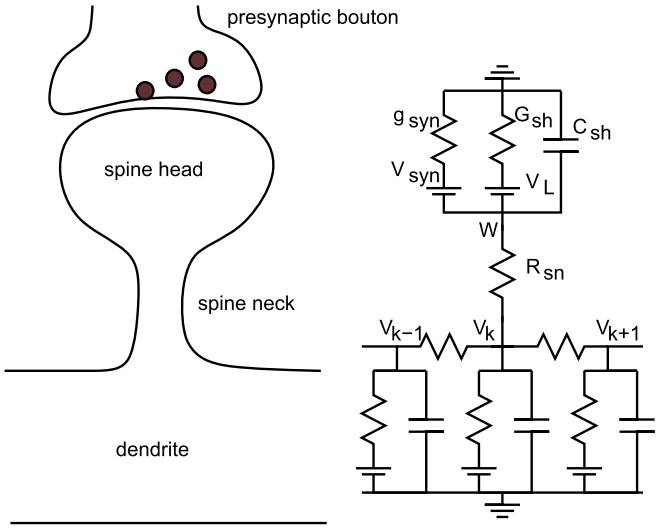

FIGURE 6.9 A schematic of synaptic contact onto the head of a spine emanating from compartment k of our discrete cable, and its associated circuit diagram. The red circles are synaptic vesicles. Depolarization of the presynaptic bouton causes one or more of these vesicles to fuse with the plasma membrane and deliver their payload of neurotransmitter to the synaptic cleft. Upon diffusion across the cleft the neurotransmitter then gates ion channels on the spine head.

where $\overline{g}_{syn}$ is in mS and ρ_{syn} is the number of conductances per unit area. With $w \equiv W - V_{Cl}$ and

$$c_{syn}(t) = g_{syn}(t)/G_{sh}, \quad \text{and} \quad \gamma_1 = 1/(R_{sn}G_{sh}) \quad \text{and} \quad \gamma_2 = 1/(R_{sn}2\pi a g_{Cl})$$

current balance at the spine head reads

$$\tau w'(t) + w(t) + c_{syn}(t)(w(t) - v_{syn}) = \gamma_1(v(x_s,t) - w(t)) \tag{6.59}$$

while the associated cable equation reads

$$\tau \frac{\partial v}{\partial t}(x,t) + v(x,t) - \lambda^2 \frac{\partial^2 v}{\partial x^2}(x,t) = \gamma_2(w(t) - v(x,t))\delta(x - x_s). \tag{6.60}$$

To solve this coupled cable/spine system we first apply the trapezoid rule to the spine equation, Eq. (6.59), finding

$$\mathtt{w}^j = \frac{(2\tau/dt - 1 - c_{syn}^{j-1} - \gamma_1)\mathtt{w}^{j-1} + v_{syn}(c_{syn}^{j-1} + c_{syn}^{j}) + (\mathtt{v}_k^{j-1} + \mathtt{v}_k^{j})\gamma_1}{2\tau/dt + 1 + c_{syn}^{j} + \gamma_1} \tag{6.61}$$

and then apply the trapezoid rule to the cable equation, Eq. (6.60), bringing

$$((2/dt)\mathbf{I} - \mathbf{B} + \gamma_2 \mathbf{e}_k \mathbf{e}_k^T)\mathtt{v}^j = ((2/dt)\mathbf{I} + \mathbf{B} - \gamma_2 \mathbf{e}_k \mathbf{e}_k^T)\mathtt{v}^{j-1} + \gamma_2(\mathtt{w}^j + \mathtt{w}^{j-1})\mathbf{e}_k. \tag{6.62}$$

The latter suggests that we compile

$$\mathtt{w}^j + \mathtt{w}^{j-1} = \frac{(4\tau/dt + c_{syn}^{j} - c_{syn}^{j-1})\mathtt{w}^{j-1} + v_{syn}(c_{syn}^{j-1} + c_{syn}^{j}) + (\mathtt{v}_k^{j-1} + \mathtt{v}_k^{j})\gamma_1}{2\tau/dt + 1 + c_{syn}^{j} + \gamma_1}.$$

This now permits us to write Eq. (6.62) as

$$((2/dt)\mathbf{I} - \mathbf{B} + \xi^j \mathbf{e}_k \mathbf{e}_k^T)\mathtt{v}^j = ((2/dt)\mathbf{I} + \mathbf{B} - \xi^j \mathbf{e}_k \mathbf{e}_k^T)\mathtt{v}^{j-1} + \mathbf{f}^j \tag{6.63}$$

where

$$\xi^j = \gamma_2 - \frac{\gamma_1\gamma_2}{2\tau/dt + 1 + c_{syn}^{j} + \gamma_1} \quad \text{and} \quad \mathbf{f}^j = \gamma_2 \frac{(4\tau/dt + c_{syn}^{j} - c_{syn}^{j-1})\mathtt{w}^{j-1} + v_{syn}(c_{syn}^{j-1} + c_{syn}^{j})}{2\tau/dt + 1 + c_{syn}^{j} + \gamma_1}\mathbf{e}_k.$$

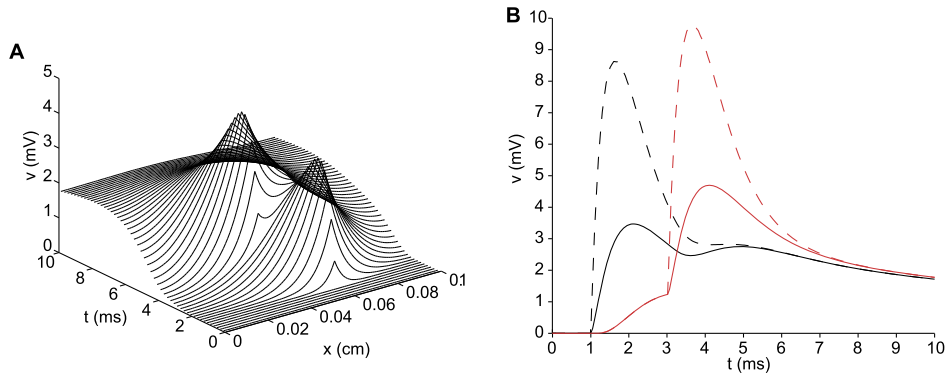

FIGURE 6.10 Response of the passive cable to two α-function synaptic inputs at spines with $\overline{g}_{syn} = 100$ nS, $\tau_\alpha = 1/2$ ms at $x = 0.06$ cm at $t_1 = 1$ ms and at $x = 0.04$ cm at $t_1 = 3$ ms. **A**. The full space–time response. **B**. The time response at the early site, $x = 0.06$ cm (black), and the late site, $x = 0.04$ cm, (red). The solid curves depict the cable potential, $v(x_s, t)$, at that site while the dashed ones depict spine head potential, $\mathtt{w}(t)$. The spine increases the input resistance at x_s and so amplifies $\mathtt{w}$ over v. This may have important consequences for active channels in the spine head. (`trapcabspine.m`)

Arguing as above, we initialize $\mathtt{v}^1 = \mathtt{w}^1 = 0$, evaluate $\mathbf{f}^2$, set $\mathbf{r}^2 = \mathbf{f}^2$ and solve

$$((2/dt)\mathbf{I} - \mathbf{B} + \xi^2 \mathbf{e}_k \mathbf{e}_k^T)\mathtt{v}^2 = \mathbf{f}^2$$

for $\mathtt{v}^2$. We then evaluate Eq. (6.61) for $\mathtt{w}^2$, set

$$\mathbf{r}^j \equiv ((4/dt)\mathbf{I} + (\xi^{j-1} - \xi^j)\mathbf{e}_k \mathbf{e}_k^T)\mathtt{v}^{j-1} - \mathbf{r}^{j-1} + \mathbf{f}^j, \quad j = 3, 4, \ldots$$

and solve

$$((2/dt)\mathbf{I} - \mathbf{B} + \xi^j \mathbf{e}_k \mathbf{e}_k^T)\mathtt{v}^j = \mathbf{r}^j \quad j = 3, 4, \ldots$$

Finally, we solve Eq. (6.61) for $\mathtt{w}^j$ and repeat. We have coded this in `trapcabspine.m` and illustrate it in Figure 6.10.

6.6 SUMMARY AND SOURCES

We derived the discrete passive cable equation and expressed its solution, when driven by current injected at a single compartment, in terms of the eigenvalues and eigenvectors of the associated second difference matrix. The expression is simply a weighted sum of convolutions familiar from our single compartment work – where the weights are eigenvectors and the constituents of the convolutions are the current stimulus and exponentials with decay rates parametrized by the eigenvalues. This representation persists as the number of compartments grows. In fact, it is the limiting case that permits exact, closed form, solution. In the case that input is delivered through changes in conductance rather than direct current injection our analytical techniques become unwieldy and we return to the trapezoid rule to build a time marching approximation scheme. This scheme permitted us to explore the interaction of synaptic input onto distinct spines.

Dendritic Cable Theory was developed by Wilfrid Rall, see Rall and Agmon-Snir (1998) for a modern survey and Segev et al. (1994) for the original papers. We have argued that the eigenvectors of the second difference matrix, $\mathbf{S}$, and eigenfunctions of the second order differential operator, ∂_{xx}, permit us to represent the response of the cable to current stimuli. We will see in Exercise 16, that these eigenvectors, and values, also permit us to analyze the performance of the associated approximation schemes. The separation of space and time variables executed in §6.4 was pioneered by Fourier, Sturm and Liouville. We will hear more from Fourier in Chapter 7. Redheffer and Port (1992) provides an excellent introduction to Sturm–Liouville theory. The cable equation is an instance of the well studied heat, or diffusion, equation. As such, there exist a number of alternate approaches, for example Green's functions, that have been exploited by neuroscientists. We recommend Strauss (2007) for the mathematics and Tuckwell (1988b) for the applications. The spine model of §6.5 is drawn from Baer and Rinzel (1991). For a rigorous presentation of

the perturbation argument invoked in Exercise 4 to prove that **every** symmetric matrix in $\mathbb{R}^{N\times N}$ has N orthonormal eigenvectors, see §17.3 in Redheffer and Port (1992). For a deeper look at the Cholesky Decomposition of Exercise 5 see Golub and van Loan (1996). The Weierstrass M-test for uniform convergence, Eq. (6.75), is proven in Redheffer and Port (1992). The determination of the cable parameters in Exercise 9 from moments of the end potential and current is drawn from Cox (1998). The summation identities, Eqs. (6.67), (6.70) and (6.73) are consequences of the Residue Theorem, see Spiegel et al. (2009).

6.7 EXERCISES

1. Show that the N-by-N second difference matrix, S, is negative semidefinite by confirming the identity
$$\mathbf{u}^T\mathbf{S}\mathbf{u} = -\sum_{j=1}^{N-1}(u_j - u_{j+1})^2/dx^2.$$
2. Prove that the eigenvalues of a real symmetric matrix are real by following these steps. Suppose $\mathbf{A} = \mathbf{A}^T$ is real and that
$$\mathbf{A}\mathbf{u} = z\mathbf{u}. \tag{6.64}$$
(i) Take the complex conjugate of each side and arrive at
$$\mathbf{A}\mathbf{u}^* = z^*\mathbf{u}^*. \tag{6.65}$$
(ii) Multiply (6.64) by $\mathbf{u}^H \equiv (\mathbf{u}^*)^T$ and (6.65) by $\mathbf{u}^T$, and take the difference of the two resulting products and use the symmetry of $\mathbf{A}$ to reduce this difference to $0 = z - z^*$.
3. †Prove that the eigenvalues of a symmetric negative semidefinite matrix are nonpositive. *Hint*: write $\mathbf{A}\mathbf{u} = z\mathbf{u}$ and multiply each side by $\mathbf{u}^T$.
4. †(i) Prove that the eigenvectors, associated with distinct eigenvalues, of a symmetric matrix are orthogonal to one another by following these steps. Write $\mathbf{A}\mathbf{u}_1 = z_1\mathbf{u}_1$ and $\mathbf{A}\mathbf{u}_2 = z_2\mathbf{u}_2$ and suppose that $z_1 \neq z_2$. Now as above, multiply the former by $\mathbf{u}_2^T$ and the latter by $\mathbf{u}_1^T$, take the difference of the products and conclude that $0 = (z_1 - z_2)\mathbf{u}_1^T\mathbf{u}_2$.
(ii) In the case that $\mathbf{A}$ does not possess distinct eigenvalues we note $\mathbf{A}$ must be very close to a symmetric matrix that does possess distinct eigenvalues. For example, the double eigenvalue of the 2×2 identity matrix stems from the degenerate characteristic polynomial $(1-z)^2$ and is easily split by perturbing $\mathbf{I}$ to
$$\mathbf{I}_\varepsilon \equiv \begin{pmatrix} 1 & \varepsilon \\ \varepsilon & 1 \end{pmatrix}.$$
Compute, by hand, its eigenvalues and eigenvectors and show that they converge, as $\varepsilon \to 0$, to the eigenvalue, and two orthogonal eigenvectors, of the 2×2 identity matrix.
5. †Given $\mathbf{A}\mathbf{u} = z\mathbf{u}$ and 2 constants, α and β, show that $\mathbf{u}$ is also an eigenvector of $\alpha\mathbf{I} + \beta\mathbf{A}$ and that $\alpha + \beta z$ is the associated eigenvalue. If $\mathbf{A}$ is also invertible explain how the eigenvalues and eigenvectors of $\mathbf{A}^{-1}$ may be determined by those of $\mathbf{A}$.
6. Use Eq. (6.13) to show that the $\mathbf{Q}$ defined in Eq. (6.15) indeed obeys $\mathbf{Q}^T = \mathbf{Q}^{-1}$.
7. If $\mathbf{A}$ is symmetric and positive definite then its LU factorization, recall Exercise 5.2, simplifies to $\mathbf{A} = \mathbf{L}\mathbf{L}^T$ where $\mathbf{L}$ is lower triangular, but not necessarily with ones on its diagonal. $\mathbf{A} = \mathbf{L}\mathbf{L}^T$ is known as the Cholesky Factorization.
(i) Show that any $\mathbf{A}$ may be written $\mathbf{A} = \mathbf{L}\mathbf{D}\mathbf{U}$ where $\mathbf{L}$ is lower triangular, $\mathbf{D}$ is diagonal, $\mathbf{U}$ is upper triangular and both $\mathbf{L}$ and $\mathbf{U}$ haves ones on their diagonal.
(ii) If $\mathbf{A} = \mathbf{A}^T$ show that $\mathbf{L}\mathbf{D}\mathbf{U} = \mathbf{U}^T\mathbf{D}\mathbf{L}^T$ and then $\mathbf{L}^{-1}\mathbf{U}^T\mathbf{D} = \mathbf{D}\mathbf{U}\mathbf{L}^{-T}$.
(iii) Observe, in this last equation, that the left is lower while the right is upper and so conclude that each side is diagonal. Given ones on the diagonals of $\mathbf{L}$ and $\mathbf{U}$ establish in fact that $\mathbf{L}^{-1}\mathbf{U}^T\mathbf{D} = \mathbf{D}$ and conclude that $\mathbf{U} = \mathbf{L}^T$ and $\mathbf{A} = \mathbf{L}\mathbf{D}\mathbf{L}^T$.

(iv) If, in addition, $\mathbf{A}$ is positive definite conclude that each element of $\mathbf{D}$ is positive and so $\mathbf{D} = \mathbf{D}^{1/2}\mathbf{D}^{1/2}$ and $\mathbf{A} = (\mathbf{L}\mathbf{D}^{1/2})(\mathbf{L}\mathbf{D}^{1/2})^T$.

8. †Suppose that $\mathbf{A} \in \mathbb{R}^{n\times n}$ is symmetric and positive definite. If λ_1 and λ_n are its largest and smallest eigenvalues, respectively, then show that

$$\lambda_n \mathbf{x}^T\mathbf{x} \le \mathbf{x}^T\mathbf{A}\mathbf{x} \le \lambda_1 \mathbf{x}^T\mathbf{x} \quad \forall\, \mathbf{x} \in \mathbb{R}^n.$$

9. We now generalize the moment calculations of §3.2 to the cable.
(i) First deduce from Eq. (6.45) that

$$M_0(v(0,\cdot)) = \frac{M_0(I_{stim})}{2\pi a C_m}\sum_{n=0}^{\infty}\frac{q_n^2(0)}{\zeta_n}. \tag{6.66}$$

Next define $L \equiv \ell/\lambda$ and use

$$\sum_{n=1}^{\infty}\frac{1}{c^2+n^2} = \frac{\pi}{2c}\coth(\pi c) - \frac{1}{2c^2} \tag{6.67}$$

to deduce that

$$\sum_{n=0}^{\infty}\frac{q_n^2(0)}{\zeta_n} = \frac{\tau}{\ell} + \frac{2\tau}{\ell}\sum_{n=1}^{\infty}\frac{1}{1+n^2\pi^2/L^2} = \frac{\tau}{\lambda}\coth(L)$$

and so conclude that

$$\boxed{\frac{M_0(v(0,\cdot))}{M_0(I_{stim})} = \frac{\coth(L)}{2\pi a\lambda g_{Cl}}.} \tag{6.68}$$

(ii) Deduce from Eq. (6.45) that

$$M_1(v(0,\cdot)) = \frac{M_1(I_{stim})}{2\pi a C_m}\sum_{n=0}^{\infty}\frac{q_n^2(0)}{\zeta_n} + \frac{M_0(I_{stim})}{2\pi a C_m}\sum_{n=0}^{\infty}\frac{q_n^2(0)}{\zeta_n^2} \tag{6.69}$$

and use

$$\sum_{n=1}^{\infty}\frac{1}{(c^2+n^2)^2} = \frac{\pi^2 c + \pi\cosh(\pi c)\sinh(\pi c)}{4c^3\sinh^2(\pi c)} - \frac{1}{2c^4} \tag{6.70}$$

to evaluate

$$\sum_{n=0}^{\infty}\frac{q_n^2(0)}{\zeta_n^2} = \frac{\tau^2}{\ell}\left\{1 + 2\frac{L^4}{\pi^4}\sum_{n=1}^{\infty}\frac{1}{((L/\pi)^2+n^2)^2}\right\} = \frac{\tau^2}{\lambda}\frac{L+\cosh(L)\sinh(L)}{2\sinh^2(L)}$$

and so arrive at

$$\boxed{\frac{M_1(v(0,\cdot))}{M_0(v(0,\cdot))} - \frac{M_1(I_{stim})}{M_0(I_{stim})} = \frac{\tau}{2}\left(1 + \frac{2L}{\sinh(2L)}\right).} \tag{6.71}$$

(iii) Finally, deduce from Eq. (6.45) that

$$M_2(v(0,\cdot)) = \frac{M_2(I_{stim})}{2\pi a C_m}\sum_{n=0}^{\infty}\frac{q_n^2(0)}{\zeta_n} + \frac{M_1(I_{stim})}{\pi a C_m}\sum_{n=0}^{\infty}\frac{q_n^2(0)}{\zeta_n^2} + \frac{M_0(I_{stim})}{\pi a C_m}\sum_{n=0}^{\infty}\frac{q_n^2(0)}{\zeta_n^3} \tag{6.72}$$

and use

$$\sum_{n=1}^{\infty} \frac{1}{(c^2+n^2)^3} = \frac{3\pi^2 c + 2\pi^3 c^2 \coth(\pi c) + (3/2)\sinh(2\pi c)}{16 c^5 \sinh^2(\pi c)} - \frac{1}{2c^6} \tag{6.73}$$

to evaluate

$$\sum_{n=0}^{\infty} \frac{q_n^2(0)}{\zeta_n^3} = \frac{\tau^3}{\lambda} \frac{3L + 2L^2\coth(L) + (3/2)\sinh(2L)}{8\sinh^2(L)}.$$

Use this expression together with (6.68) and (6.71) to write a single equation for L, namely

$$F(L) = \frac{M_2(v_0)/M_0(v_0) - M_2(I)/M_0(I) - 2\tau_c(I)(\tau_c(v_0) - \tau_c(I))}{(\tau_c(v_0) - \tau_c(I))^2}$$

where

$$F(L) \equiv \frac{\sinh^2(2L)}{(\sinh(2L)+2L)^2} \frac{3L\tanh(L) + 2L^2 + 3\sinh^2(L)}{\sinh^2(L)}.$$

It follows that the first 3 moments of the stimulus and response uniquely determine L if their combination above strikes F where it is monotone. Over what interval is F monotone?

10. †Develop both $f(x+dx)$ and $f(x-dx)$ in Taylor series about x. Add these two series and conclude that

$$\frac{f(x+dx) - 2f(x) + f(x-dx)}{dx^2} \to f''(x) \quad \text{as} \quad dx \to 0.$$

This justifies our passage from (6.29) to (6.30).

11. To solve the steady-state cable equation, (6.32), we attempt the educated (linear equations are solved by exponentials) guess $v_\infty(x) = e^{\alpha x}$.
(i) Insert this guess into (6.32), find that $\alpha = \pm 1/\lambda$, and deduce that $v_\infty(x) = c_1 e^{x/\lambda} + c_2 e^{-x/\lambda}$.
(ii) Determine the values of the two constants c_1 and c_2 from the boundary conditions, (6.33).
(iii) Confirm that your answer agrees with (6.34) where

$$\sinh(x) = \frac{e^x - e^{-x}}{2} \quad \text{and} \quad \cosh(x) = \frac{e^x + e^{-x}}{2}.$$

Plot (6.34) and compare with Figure 6.3.

12. †We approach the eigenvalue problem, (6.37), via the same tack as that of the previous exercise.
(i) Attempt $q(x) = \exp(\alpha x)$ and show that $q(x) = c_1 \exp(\sqrt{\vartheta}x) + c_2 \exp(-\sqrt{\vartheta}x)$.
(ii) Show that $q'(0) = 0$ translates into $c_1 = c_2$ while $q'(\ell) = 0$ requires that $\exp(2\sqrt{\vartheta}\ell) = 1$. Argue that this requires $2\sqrt{\vartheta}\ell = i2\pi n$ for $n = 0, 1, 2, \ldots$ and conclude that $\vartheta = -(n\pi/\ell)^2$.

13. Regarding the convergence of the infinite sum in Eq. (6.45), suppose that $I_{stim}^{max} = \max\{|I_{stim}(s)|; 0 \le s \le \infty\}$ and show that

$$\left| \int_0^t I_{stim}(s) \exp((t-s)\zeta_n)\, ds \right| \le I_{stim}^{max} \int_0^t \exp((t-s)\zeta_n)\, ds \le \frac{\tau I_{stim}^{max}}{1 + (n\pi(\lambda/\ell))^2}. \tag{6.74}$$

Deduce from Eq. (6.67) that this sequence is summable. Finally, invoke the
Weierstrass M-test: If each $v_n(x,t)$ obeys $\max\{|v_n(x,t)| : x \in [0,\ell], 0 \le t\} \le M_n$ and M_n is summable then there exists a function $v(x,t)$ such that given any $\varepsilon > 0$ there exists an index N such that

$$\max_{x\in[0,\ell], 0\le t} \left| v(x,t) - \sum_{n=1}^{m} v_n(x,t) \right| \le \varepsilon \tag{6.75}$$

whenever $m \ge N$.

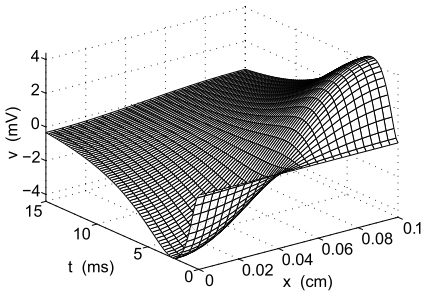

FIGURE 6.11 The graph of the v in (6.81) using passive parameters defined in Eq. (6.17). (`pfibexact.m`)

to conclude that the sum in Eq. (6.45) indeed converges. In this case we say that the sum of the v_n converges uniformly to v. As each v_n is continuous it then follows that so too is v, and although integrals of the v_n will sum to integrals of v the same cannot be said for derivatives. To see this, differentiate each side of Eq. (6.45) with respect x and then set $x = 0$.

14. We now show that our analytical methods are general enough to accommodate an arbitrary spatio-temporal current stimulus, I (μA/cm). In particular, solve

$$\tau \frac{\partial v}{\partial t}(x,t) + v(x,t) - \lambda^2 \frac{\partial^2 v}{\partial x^2}(x,t) = I(x,t)/(2\pi a g_{Cl}), \tag{6.76}$$

subject to $v_x(0,t) = v_x(\ell,t) = v(x,0) = 0$ by mimicking our separation of variables argument. First show that p_n obeys

$$\tau p_n'(t) + (1 + \lambda^2 \vartheta_n) p_n(t) = I_n(t)/(2\pi a g_{Cl}), \quad p_n(0) = 0, \tag{6.77}$$

where

$$I_n(t) = \int_0^\ell I(x,t) q_n(x)\, dx. \tag{6.78}$$

You should then arrive at

$$v(x,t) = \sum_{n=0}^{\infty} \frac{q_n(x)}{C_m 2a\pi} \int_0^t I_n(s) \exp((t-s)\zeta_n)\, ds. \tag{6.79}$$

Please show that if

$$I(x,t) = -\sqrt{2/\ell} \cos(\pi x/\ell)(e^{-t} - e^{-2t})/500 \tag{6.80}$$

then v is simply

$$v(x,t) = -\frac{\sqrt{2/\ell}\cos(\pi x/\ell)}{C_m 2a\pi} \frac{e^{-t}(\zeta_1 - 2) + e^{-2t}(1-\zeta_1) + e^{-\zeta_1 t}}{500(\zeta_1 - 1)(\zeta_1 - 2)}. \tag{6.81}$$

Use `meshgrid` and `mesh` to illustrate this solution as in Figure 6.11.

15. We show that our moment methods allow us to ascertain the location of synaptic input from indirect measurements. In particular, we suppose that v obeys Eq. (6.53) with sealed ends and that we have recorded both end potentials, $v(0,t)$ and $v(\ell,t)$.
(i) Define the left and right moments

$$M_L(x) \equiv \int_0^\infty v(x,t)\, dt, \quad 0 \le x \le x_s \quad \text{and} \quad M_R(x) \equiv \int_0^\infty v(x,t)\, dt, \quad x_s \le x \le \ell$$

and use Eq. (6.53) to conclude that $\lambda^2 M_L''(x) = M_L(x)$ and $\lambda^2 M_R''(x) = M_R(x)$.
(ii) Using known information about M_L at $x = 0$ and M_R at $x = \ell$ show that

$$M_L(x) = M_0(v(0,\cdot))\cosh(x/\lambda) \quad \text{and} \quad M_R(x) = M_0(v(\ell,\cdot))\cosh((\ell - x)/\lambda).$$

(iii) Explain why $M_L(x_s) = M_R(x_s)$ and use this to derive the following equation for x_s,

$$\sigma(x_s) \equiv \frac{\cosh((\ell - x_s)/\lambda)}{\cosh(x_s/\lambda)} = \frac{M_0(v(0,\cdot))}{M_0(v(\ell,\cdot))}. \tag{6.82}$$

Demonstrate that σ is a monotone function of x_s and hence that the end moments uniquely determine the site of synaptic input.

16. Let us investigate the stability of the unforced (i.e., without current or synaptic inputs) forward Euler scheme

$$\mathsf{v}^j = (\mathbf{I} + dt\mathbf{B})\mathsf{v}^{j-1}.$$

As above, it follows that $\mathsf{v}^j = (\mathbf{I} - dt\mathbf{B})^{j-1}\mathsf{v}^1$ and so we look for a condition on dt that will guarantee that $(\mathbf{I} - dt\mathbf{B})^{j-1}$ remains bounded. We label this forward Euler matrix

$$\mathbf{F} \equiv \mathbf{I} + dt\mathbf{B} = \mathbf{I} + (dt/\tau)(\lambda^2\mathbf{S} - \mathbf{I})$$

and deduce from Exercise 5 that $\mathbf{F}\mathbf{q}_n = \gamma_n\mathbf{q}_n$ where the $\mathbf{q}_n$ are the eigenvectors of $\mathbf{S}$ and

$$\gamma_n = 1 + (dt/\tau)(\lambda^2\theta_n - 1).$$

Show that if $\mathbf{\Gamma} = \mathtt{diag}(\gamma)$ then $\mathbf{F}\mathbf{Q} = \mathbf{Q}\mathbf{\Gamma}$ and moreover that

$$\mathbf{F} = \mathbf{Q}\mathbf{\Gamma}\mathbf{Q}^T. \tag{6.83}$$

We are now prepared to study powers of $\mathbf{F}$. Use (6.83) to show that

$$\mathbf{F}^{j-1} = \mathbf{Q}\mathbf{\Gamma}^{j-1}\mathbf{Q}^T$$

and note that to raise a diagonal matrix to a power is simply to raise each of its elements to that power. Argue then that forward Euler is stable so long as $|\gamma_{N-1}|$, the magnitude of the largest eigenvalue of $\mathbf{F}$, is less than 1. Use Eq. (6.52) to derive an explicit stability bound for dt.

17. †Few cables are uniform in shape. Most branches taper with distance from their cell body. In the compartmental case, if the radius of compartment n is a_n please show that the current balance, Eq. (6.5), takes the form

$$\frac{a_{n-1}^2 v_{n-1} - (a_{n-1}^2 + a_n^2)v_n + a_n^2 v_{n+1}}{2R_a dx^2} = a_n(C_m v_n' + g_{Cl}v_n). \tag{6.84}$$

Next show, that as $dx \to 0$ and $n \to \infty$ this takes the form of the tapered cable equation

$$\frac{\partial}{\partial x}\left(a^2(x)\frac{\partial v}{\partial x}(x,t)\right) = 2R_a a(x)\{C_m\frac{\partial v}{\partial t}(x,t) + g_{Cl}v(x,t)\}. \tag{6.85}$$